Molecular Pharmacology Fast Forward. Published on June 6, 2007 as doi:10.1124/mol.107.034413
This article has not been copyedited and formatted. The final version may differ from this version.

MOL #34413

Molecular analysis of the interaction of *Bordetella pertussis* adenylyl cyclase with fluorescent nucleotides[†]

Martin Göttle, Stefan Dove, Phillip Steindel, Yuequan Shen,

Wei-Jen Tang, Jens Geduhn, Burkhard König and Roland Seifert[1]

Department of Pharmacology and Toxicology (M.G., P.S., R.S.) and Department of Pharmaceutical and Medicinal Chemistry II (S.D.), Institute of Pharmacy, University of Regensburg, Germany; Ben May Department for Cancer Research, The University of Chicago (W.-J.T.); The College of Life Sciences, Nankai University, China (Y.S.); Institute of Organic Chemistry, University of Regensburg, Germany (J.G., B.K.)

Molecular Pharmacology Fast Forward. Published on June 6, 2007 as DOI: 10.1124/mol.107.034413
This article has not been copyedited and formatted. The final version may differ from this version.

MOL #34413

Running title

Molecular analysis of *Bordetella pertussis* adenylyl cyclase

[1]Corresponding author

Dr. Roland Seifert

Department of Pharmacology and Toxicology, Institute of Pharmacy,

University of Regensburg

Universitaetsstr. 31

D-93053 Regensburg, Germany

Telephone: +49-941-943-4770. Fax: +49-941-943-4772.

E-mail: roland.seifert@chemie.uni-regensburg.de

Number of text pages: 36

Number of Tables: 1

Number of Figures: 6

Number of References: 28

Number of words in Abstract: 241

Number of words in Introduction: 703

Number of words in Discussion: 1488

Abbrevations

AC, adenylyl cyclase; ANT, anthraniloyl-; CaM, calmodulin; CyaA, *Bordetella pertussis* adenylyl cyclase; FRET, fluorescence resonance energy transfer; MANT, methylanthraniloyl-; NDP, nucleoside 5´-diphosphate; NTP, nucleoside 5´-triphosphate; PMEApp, 9-[2-(phosphonomethoxy)ethyl]adenine diphosphate; TNP, 2,4,6-trinitrophenyl-.

Molecular Pharmacology Fast Forward. Published on June 6, 2007 as DOI: 10.1124/mol.107.034413
This article has not been copyedited and formatted. The final version may differ from this version.

Abstract

The calmodulin (CaM)-dependent adenylyl cyclase (AC) toxin from *Bordetella pertussis* (CyaA) substantially contributes to the pathogenesis of whooping cough. Thus, potent and selective CyaA inhibitors may be valuable drugs for prophylaxis of this disease. We examined the interactions of fluorescent 2´,3´-*N*-methylanthraniloyl (MANT)-, anthraniloyl- and trinitrophenyl (TNP)-substituted nucleotides with CyaA. Compared to mammalian AC isoforms and *Bacillus anthracis* AC toxin edema factor, nucleotides inhibited catalysis by CyaA less potently. Introduction of the MANT substituent resulted in 5 to 170-fold increased potency of nucleotides. K_i-values of 3'MANT-2'd-ATP and 2'MANT-3'd-ATP in the AC activity assay using Mn^{2+} were 220 nM and 340 nM, respectively. Natural nucleoside 5'-triphosphates, guanine-, hypoxanthine- and pyrimidine-MANT- and TNP-nucleotides and di-MANT-nucleotides inhibited CyaA, too. MANT-nucleotide binding to CyaA generated fluorescence resonance energy transfer (FRET) from tryptophans W69 and W242 and multiple tyrosine residues, yielding K_d-values of 300 nM for 3´MANT-2´d-ATP and 400 nM for 2´MANT-3´d-ATP. Fluorescence experiments and docking approaches indicate that the MANT- and TNP groups interact with F306. Increases of FRET and direct fluorescence with MANT-nucleotides were strictly CaM-dependent, whereas TNP-nucleotide fluorescence upon binding to CyaA increased in the absence of CaM and was actually reduced by CaM. In contrast to low-affinity MANT-nucleotides, even low-affinity TNP-nucleotides generated strong fluorescence increases upon binding to CyaA. We conclude that the catalytic site of CyaA possesses substantial conformational freedom to accommodate structurally diverse ligands and that certain ligands bind to CyaA even in the absence of CaM, facilitating future inhibitor design.

Molecular Pharmacology Fast Forward. Published on June 6, 2007 as DOI: 10.1124/mol.107.034413
This article has not been copyedited and formatted. The final version may differ from this version.

Introduction

Bordetella pertussis toxin CyaA is a 1706-amino acid virulence factor interacting with surface receptors of eukaryotic host cells and translocating its AC domain into the cytosol (Confer and Eaton, 1982; Hewlett et al., 1989; Ladant and Ullmann, 1999). After activation by calmodulin (CaM), an endogenous calcium sensor, CyaA catalyzes massive synthesis of cAMP (Mock and Ullmann, 1993; Shen et al., 2002; Ahuja et al., 2004). cAMP inhibits phagocyte function and facilitates respiratory tract infection by *Bordetella pertussis* (Boyd et al., 2005; Carbonetti et al., 2005; Hewlett et al., 2006). Substrate analogs may be used to inhibit the catalytic activity of CyaA (Johnson and Shoshani, 1990; Soelaiman et al., 2003; Gille et al., 2004) and prophylaxis of *Bordetella pertussis* infection. Recently, we discovered *N*-methylanthraniloyl (MANT)-substituted NTPs as competitive inhibitors of mammalian and bacterial ACs including CyaA (Gille and Seifert, 2003; Gille et al., 2004). Additionally, 2´,3´-(2,4,6-trinitrophenyl) (TNP)-substituted NTPs are potent inhibitors of mammalian AC (Mou et al., 2006). Furthermore, adefovir, a drug for the treatment of chronic hepatitis B virus infection, is a potent CyaA inhibitor (Shen et al., 2004).

Mammals express nine membranous AC isoforms (ACs 1-9) and a soluble AC. We have employed the cytosolic catalytic domains C1 of type 5 AC and C2 of type 2 AC for molecular AC analysis (Gille et al., 2004; Mou et al., 2005, 2006). Comparing the crystal structures of C1:C2 bound to MANT-GTP, MANT-ATP and TNP-ATP, we found the catalytic site of AC to consist of three binding pockets, accommodating the base, the 2´,3´-ribosyl substituent and the phosphate chain. We have also reported the crystal structure of CyaA in complex with CaM and 9-[2-(phosphonomethoxy)ethyl]adenine diphosphate (PMEApp), the active metabolite of adefovir (Guo et al., 2005). Forty-nine amino acid residues of CyaA and 41 residues of CaM form salt bridges, hydrogen bonds and hydrophobic contacts, resulting in

Molecular Pharmacology Fast Forward. Published on June 6, 2007 as DOI: 10.1124/mol.107.034413
This article has not been copyedited and formatted. The final version may differ from this version.

high affinity of CyaA for CaM (K_d = 0.2 nM). However, the precise conformational changes in the catalytic site of CyaA underlying its activation by CaM are still unknown. An understanding of these processes will greatly facilitate future inhibitor design.

In order to monitor nucleotide binding to, and conformational changes in, CyaA, several different approaches can be employed. Firstly, MANT- and ANT-nucleotides are environmentally sensitive probes displaying increased fluorescence and blue-shift of the emission maximum upon exposure to a hydrophobic environment (Hiratsuka, 1983; Jameson and Eccleston, 1997). As is obvious from the CyaA crystal structure in complex with PMEApp (Guo et al., 2005), the catalytic site contains the hydrophobic residue F306. Nucleotide binding to CyaA allows hydrophobic interactions between the MANT/ANT-group and F306, resulting in an increased fluorescence signal (Sarfati et al., 1990; Guo et al., 2005). This notion is supported by the fact that CyaA-F306A does not increase the fluorescence signal of 3´ANT-2´d-ATP (Guo et al., 2005). Secondly, the catalytic domain of CyaA bears two tryptophan residues, W69 located 21 Å and W242 38 Å away from the catalytic site (Guo et al., 2005). These distances allow fluorescence resonance energy transfer (FRET) (Lakowicz, 1999) from tryptophan (excitation wavelength of 280 nm and emission wavelength of 350 nm) to MANT (excitation wavelength of 350 nm and emission wavelength of 450 nm) (Gilles et al., 1990; Mou et al., 2005, 2006). Thirdly, TNP-nucleotides are environmentally sensitive fluorescence probes, too (Hiratsuka, 2003). Like MANT-nucleotides, TNP-nucleotides show a blue-shift in emission in a hydrophobic environment (Hiratsuka, 2003). Compared to MANT/ANT-nucleotides, TNP-nucleotides are more rigid since the fluorophore is attached through both the 2'- and 3'-ribosyl position, avoiding potential problems with fluorophore isomerization (Jameson and Eccleston, 1997; Hiratsuka, 2003). A potential advantage of TNP-

Molecular Pharmacology Fast Forward. Published on June 6, 2007 as DOI: 10.1124/mol.107.034413
This article has not been copyedited and formatted. The final version may differ from this version.

nucleotides compared to MANT-nucleotides is the fact that the relative fluorescence increases can be substantially larger, depending on the specific protein studied (Jameson and Eccleston, 1997; Hiratsuka, 2003; Mou et al., 2005, 2006).

In the present study, we used MANT/ANT- and TNP-nucleotides as probes to determine their potencies at inhibiting CyaA and to investigate conformational changes in the catalytic site. Nucleotides **12**, **14**, **15**, **18**, **19**, **20**, **25**, **30** and **31** represent newly synthesized fluorescent probes. Moreover, the binding mode of nucleotides was explored by docking of representative derivatives to a CyaA model derived from the crystal structure in complex with PMEApp (Shen et al., 2004; Guo et al., 2005).

Molecular Pharmacology Fast Forward. Published on June 6, 2007 as DOI: 10.1124/mol.107.034413
This article has not been copyedited and formatted. The final version may differ from this version.

Materials and Methods

Materials. MANT- and ANT-substituted NTPs of adenosine, cytidine, inosine and uridine were synthesized according to a documented procedure (Hiratsuka, 1983). The modification of the synthesis by lowering the pH-value from 9.6 to 8.6 induced higher yields. In case of the starting material methyl-isatoic anhydride, the major portion of the excessive compound was removed by $CHCl_3$-extraction. In general, the separation of starting materials could be achieved by using size exclusion chromatography with Sephadex® LH–20 in water. However, HPLC-analysis and liquid chromatography/mass spectrometry coupling still showed by-product of the corresponding (M)ANT-diphosphate residue. Pure MANT-nucleotides were obtained by preparative reversed-phase HPLC with a Phenomenex Luna C18(2) column (particle size: 10 µm, length: 250 mm, inner diameter: 21.2 mm). The nucleoside 5'-diphosphates were also collected because of their putative inhibitory effects. (M)ANT-nucleoside 5'-diphosphates and triphosphates were obtained in high purity of 99%. Di-MANT-IMP (**31**) bearing two MANT-groups at the 2´,3´-ribosyl position was also found as a by-product of our synthesis and was purified to 99% content, too.

MANT-ATP (**8**), MANT-GTP (**10**), ANT-GTP (**24**), 3'MANT-2'd-ATP (**21**), 2'MANT-3'd-ATP (**22**), TNP-CTP (**28**), TNP-UTP (**29**) and γS-substituted MANT-nucleotides (**9**, **11**, **13**) were obtained from Jena Bioscience, Jena, Germany. In case of MANT-ATP, the MANT-group isomerizes between the 2´ and 3´ position of the ribose ring, whereas in 2'MANT-3'd-ATP and 3'MANT-2'd-ATP the MANT-group is fixed to the corresponding position due to the absence of the neighboring hydroxyl group. PMEApp (**1**) was supplied by Gilead Sciences, Foster City, CA. TNP-ATP (**26**) and TNP-GTP (**27**) were from Molecular Probes, Eugene, OR. ITP was from Sigma-Aldrich, Seelze, Germany; GTP was from Roche, Mannheim, Germany. UTP and CTP were from Boehringer, Ingelheim, Germany. The catalytic domain of *Bordetella*

Molecular Pharmacology Fast Forward. Published on June 6, 2007 as DOI: 10.1124/mol.107.034413
This article has not been copyedited and formatted. The final version may differ from this version.

pertussis AC protein (CyaA, amino acids 1 to 373) was purified as described (Shen et al., 2002). Lyophilized calmodulin from bovine brain was purchased from EMD Biosciences, Calbiochem, Darmstadt, Germany. [α–^{32}P]ATP (800 Ci/mmol) was purchased from PerkinElmer, Wellesley, MA. Aluminum oxide 90 active, neutral (activity 1, particle size 0.06 - 0.2 mm) was purchased from Merck, Darmstadt, Germany. Albumin from bovine serum, fraction V, highest quality, was from Sigma-Aldrich. $MnCl_2$ tetrahydrate and $MgCl_2$ hexahydrate (highest quality) were from Merck.

FRET and direct fluorescence experiments with MANT-nucleotides.

Experiments were performed using a quartz UV ultra-microcuvette from Hellma, Müllheim, Germany (type 105.251-QS, light path length 3 mm, center 15 mm, total volume 70 µL). Measurements were performed in a Varian Cary Eclipse fluorescence spectrometer at a constant temperature of 25°C (instrument settings slit width 5 nm, scan rate 120 nm/min, averaging time 0.5 s, data interval 1 nm, PMT voltage 700 V). The cuvette contained at first 64 µL of 75 mM HEPES/NaOH buffer, 100 µM $CaCl_2$, 100 mM KCl and 5 mM $MnCl_2$, pH 7.4. Next, nucleotide, CyaA and CaM were added successively. The cuvette content (final volume of 70 µL) was mixed after each addition. In FRET experiments, nucleotides were used at final concentrations from 10 nM to 2 µM, and CyaA and CaM were 300 nM each. The excitation wavelength was 280 nm, and emission was scanned from 300 nm to 550 nm. In order to investigate the kinetics of CyaA interaction with MANT-nucleotides, the excitation wavelength was 280 nm and changes in fluorescence intensity were measured over time at 430 nm. Nucleotides, CyaA and CaM were applied at a final concentration of 300 nM. MANT-nucleotides were finally displaced from CyaA using PMEApp (10 nM to 3 µM). In saturation studies, independent FRET experiments were performed using MANT-

Molecular Pharmacology Fast Forward. Published on June 6, 2007 as DOI: 10.1124/mol.107.034413
This article has not been copyedited and formatted. The final version may differ from this version.

nucleotides from 10 nM to 2 µM final concentration; CyaA and CaM were 300 nM each. Saturation curves were obtained by subtracting the fluorescence intensity at 430 nm after the addition of CyaA from the maximal fluorescence (FRET) after the addition of CyaA/CaM.

In direct fluorescence experiments, MANT-nucleotides were excited at 350 nm and emission spectra were recorded from 380 nm to 550 nm. In order to obtain large increases in direct fluorescence, CyaA and CaM (both 2.4 µM final concentration) were used in excess relative to MANT-nucleotides (100 nM final concentration), ensuring complete binding of the nucleotide to CyaA. For an estimation of the hydrophobic properties of the binding site interacting with the MANT-group, direct fluorescence of the nucleotides was determined in water and in 30% (v/v) dimethyl sulfoxide.

Fluorescence studies with TNP-nucleotides. Fluorescence studies with TNP-nucleotides were essentially performed as for MANT-nucleotides with some modifications. Specifically, the concentrations of TNP-nucleotides, CyaA and CaM were 5 µM each. The higher protein concentrations were necessary to compensate for the lower quantum yield with TNP-nucleotides compared to MANT-nucleotides (Jameson and Eccleston, 1997; Hiratsuka, 2003).The excitation wavelength was 405 nm, and emission was scanned from 480 to 620 nm.

AC activity assay. For the determination of the potency of CyaA inhibitors, assay tubes contained 10 µL of inhibitor at final concentrations from 10 nM to 100 µM and 20 µL of CyaA protein (10 pM final concentration) in 75 mM HEPES/NaOH, pH 7.4, containing 0.1% (m/v) bovine serum albumin. Tubes were preincubated for 2 min at 25°C, and reactions were initiated by the addition of 20 µL of reaction mixture

Molecular Pharmacology Fast Forward. Published on June 6, 2007 as DOI: 10.1124/mol.107.034413
This article has not been copyedited and formatted. The final version may differ from this version.

consisting of the following components to yield the given final concentrations: 100 mM KCl, 10 µM free Ca^{2+}, 5 mM free Mn^{2+} or Mg^{2+}, 100 µM EGTA, 100 µM cAMP, 100 nM calmodulin. ATP was added as non-labeled substrate at a final concentration of 40 µM and as radioactive tracer [α–^{32}P]ATP (0.2 µCi/tube). For the determination of K_m and V_{max} values, 10 µM to 2 mM ATP/Mn^{2+} or ATP/Mg^{2+} were added, plus 5 mM of free Mn^{2+} or Mg^{2+}. In order to ensure linear reaction progress, tubes were incubated for 10 min at 25°C, and reactions were stopped by the addition of 20 µL of 2.2 N HCl. Denaturated protein was sedimented by a 1-min centrifugation at 12,000 x g. [^{32}P]cAMP was separated from [α–^{32}P]ATP by transferring the samples to columns containing 1.4 g of neutral alumina. [^{32}P]cAMP was eluted by the addition of 4 mL 0.1 M ammonium acetate solution, pH 7.0. Blank values were about 0.02% of the total added amount of [α–^{32}P]ATP; substrate turnover was < 3% of the total added [α–^{32}P]ATP. Samples collected in scintillation vials were filled up with 10 mL of double-distilled water and Čerenkov radiation was measured in a PerkinElmer Tricarb 2800TR liquid scintillation analyzer.

Free concentrations of divalent cations were calculated with WinMaxC (http://www.stanford.edu/~cpatton/maxc.html). K_i-values reported in Table **1** and K_d-values obtained from saturation experiments were calculated using the Prism 4.02 software (Graphpad, San Diego, CA).

Modeling of the nucleotide binding mode to CyaA. Docking studies were performed with the molecular modeling package SYBYL 7.3 (Tripos Inc., St. Louis, MO) on a Silicon Graphics Octane workstation. An initial computer model of CyaA in complex with PMEApp was generated from the PDB crystal structure 1zot (Guo et al., 2005). Hydrogens were added and AMBER_FF99 charges were assigned to the protein and the water molecules, followed by a rough pre-optimization of the model

Molecular Pharmacology Fast Forward. Published on June 6, 2007 as DOI: 10.1124/mol.107.034413
This article has not been copyedited and formatted. The final version may differ from this version.

(100 cycles) with the AMBER_FF99 force field (Cornell et al., 1995) and fixed PMEApp. The three Mg^{2+} ions received formal charges of 2. Starting conformations of 3´MANT-2´d-ATP (**21**), 2´MANT-3´d-ATP (**22**) and TNP-ATP (**26**) were derived from complexes of 3'MANT-ATP and TNP-ATP with mammalian AC (PDB structures 2gvz and 2gvd, respectively) (Mou et al., 2005, 2006). PMEApp and the ligands **21**, **22** and **26** were provided with Gasteiger-Hueckel charges. Initial docking positions resulted from superposition of roughly optimized conformations with PMEApp, allowing the modification of rotatable bonds, and from consideration of the fluorescence data (interaction of the MANT- and TNP-groups with F306). Water molecules in the catalytic site were removed. Each complex was refined in a stepwise approach. Firstly, ~50 minimization cycles with fixed ligand (AMBER_FF99 force field, steepest descent method) were performed, secondly, ~100 minimization cycles of the ligand and the surrounding (distance up to 6 Å) protein residues (Tripos force field) (Clark et al., 1989), and, thirdly, ~100 minimization cycles with fixed ligand (AMBER_FF99 force field, Powell conjugate gradient). The second and third steps were repeated with larger number of cycles until an root mean square (RMS) force of 0.05 kcal mol^{-1} $Å^{-1}$ was approached. In order to avoid overestimation of electrostatic interactions, a distance-dependent dielectric constant of 4 was applied. Molecular surfaces and lipophilic potentials (protein variant with the new Crippen parameter table (Ghose et al., 1998, Heiden et al., 1993)) were calculated and visualized by the program MOLCAD (J. Brickmann *et al.*, Technical University of Darmstadt, Germany) contained within SYBYL.

Molecular Pharmacology Fast Forward. Published on June 6, 2007 as DOI: 10.1124/mol.107.034413
This article has not been copyedited and formatted. The final version may differ from this version.

Results

Overview on nucleotide structures. We examined the inhibitory effects of 31 nucleotides on the catalytic activity of CyaA (Table **1**). Nucleotides differed from each other in base, phosphate chain length, phosphate chain substitution, and MANT, ANT or TNP substituents at the 2´,3´-ribosyl position. In compounds **8-20**, **23-25** and **30**, the MANT- or ANT-group undergoes spontaneous isomerization between the 2´- and 3´-ribosyl position (Jameson and Eccleston, 1997). In **21** and **22**, the MANT-group is fixed to the 2´- or 3´-position because the neighboring ribosyl position is deoxygenated, thus preventing isomerization. In **23-25**, an ANT-group is attached to the ribosyl residue instead of the MANT-group. Compounds **26-29** contain TNP substituents. Since the TNP-group is attached to the ribosyl ring via the 2´- and 3´-position, isomerization is not possible in TNP-nucleotides (Hiratsuka, 2003). In **31**, two MANT-substituents are attached to the 2´- and 3´-ribosyl position. In **9**, **11** and **13**, the γ-phosphate group is substituted by a γ-thiophosphate group. The potencies of the different nucleotides were determined in the AC activity assay in the presence of either Mn^{2+} or Mg^{2+}.

Structure/activity relationships under Mn^{2+}-conditions. Under Mn^{2+}-conditions, MANT-ITP (**12**) displayed the highest potency of all MANT-NTPs examined, exhibiting 7-fold higher potency than MANT-ATP (**8**). The rank order of potencies was MANT-ITP > MANT-CTP > MANT-UTP > MANT-ATP > MANT-GTP. MANT-GTP (**10**) exhibited 10-fold lower potency compared to MANT-ITP. For MANT-NDPs, the order of potency was MANT-IDP ~ MANT-ADP > MANT-CDP > MANT-UDP with MANT-IDP being 4-fold more potent than MANT-UDP. For ANT-nucleotides, the adenine base was advantageous as compared to guanine, ANT-ATP (**23**) was 22-fold more potent than ANT-GTP (**24**). Among γS-substituted MANT-

Molecular Pharmacology Fast Forward. Published on June 6, 2007 as DOI: 10.1124/mol.107.034413
This article has not been copyedited and formatted. The final version may differ from this version.

nucleotides, the rank order of potency was MANT-ATPγS > MANT-ITPγS > MANT-GTPγS with MANT-ATPγS (**9**) being 4 to 5-fold more potent than MANT-GTPγS (**11**).

TNP-ATP (**26**) was the most potent TNP-nucleotide; the rank order was TNP-ATP > TNP-CTP > TNP-GTP > TNP-UTP. Among the nucleotides bearing no fluorescent substituent at the 2´,3´-ribosyl position, GTP (**2**) displayed the highest affinity, which was 4-fold higher than the affinity of ITP (**3**) and UTP (**6**). Interestingly, the K_i constants of GTP and CTP were lower than the K_m value of the natural substrate ATP. Compared to the non-substituted NTPs, the MANT-group increased inhibitor potency 5-fold, 31-fold, 45-fold and 166-fold for MANT-GTP, MANT-CTP, MANT-UTP and MANT-ITP, respectively. The TNP-group increased inhibitory potency in case of TNP-CTP and TNP-UTP just by factors of 3 and 2, respectively, and TNP-GTP (**27**) was only slightly more potent than GTP (**2**). MANT-substituted nucleotides were 2, 3, 9 and 22 times more potent in inhibiting CyaA as compared to TNP-nucleotides (**8** vs. **26**, **10** vs. **27**, **14** vs. **28**, and **15** vs. **29**). While ANT-ATP (**23**) was 3-fold more potent than MANT-ATP (**8**), the potency of ANT-GTP (**24**) was 5-fold lower as compared to MANT-GTP (**10**).

Omission of the γ-phosphate group resulted in substantially decreased potencies at all nucleotides. Specifically, MANT-ADP (**16**) was 3-fold less potent than MANT-ATP (**8**), MANT-GDP 10-fold than MANT-GTP (Gille et al., 2004), MANT-CDP (**19**) 15-fold than MANT-CTP (**14**), MANT-UDP (**20**) 17-fold than MANT-UTP (**15**) and MANT-IDP (**18**) 18-fold than MANT-ITP (**12**). ANT-ADP (**25**) was 9-fold less potent than ANT-ATP (**23**).

Adding the γS-substitution to MANT-NTPs decreased potency of MANT-ITP 3-fold (**12** vs. **13**), increased potency of MANT-ATP 4-fold (**8** vs. **9**) and left the potency of MANT-GTP unchanged (**10** vs. **11**). Most strikingly, 3´MANT-2´d-ATP (**21**) and

Molecular Pharmacology Fast Forward. Published on June 6, 2007 as DOI: 10.1124/mol.107.034413
This article has not been copyedited and formatted. The final version may differ from this version.

2´MANT-3´d-ATP (**22**) were 22-fold and 14-fold more potent than MANT-ATP (**8**), respectively.

Structure/activity relationships under Mg^{2+}-conditions. The exchange of Mn^{2+} by Mg^{2+} increased K_m and V_{max} 14-fold and 5-fold, respectively. Inhibitory potencies of all tested nucleotides were differentially lowered when Mg^{2+} was used instead of Mn^{2+}. While the potency of MANT-GTPγS was only minimally reduced, 3´MANT-2´d-ATP and 2´MANT-3´d-ATP showed ~160-fold and ~70-fold lower potency with Mg^{2+}. The rank order of potency for MANT-substituted NTPs was MANT-GTP = MANT-ITP > MANT-CTP > MANT-UTP > MANT-ATP. While MANT-GTP (**10**) displayed the lowest potency of all MANT-NTPs under Mn^{2+}-conditions, it was – together with MANT-ITP (**12**) – the most potent MANT-NTP when Mg^{2+} was used. ANT-ATP (**23**) was 3-fold more potent than MANT-ATP (**8**) and exceeded ANT-GTP (**24**) in potency. MANT-GTPγS (**11**) was the most potent γS-substituted nucleotide tested, being 2-fold more potent than MANT-ATPγS (**9**) and 4-fold more potent than MANT-ITPγS (**13**). The introduction of the MANT-group increased the potency of CTP, UTP and GTP 7-16-fold. Most strikingly, MANT-ITP (**12**) was ~70-fold more potent than ITP (**3**). Among TNP-nucleotides, potency decreased in the order TNP-ATP, TNP-GTP, TNP-CTP, TNP-UTP. Interestingly, the TNP-group did not increase potency compared to non-substituted NTPs; potency even decreased (**2** vs. **27**, **5** vs. **28** and **6** vs. **29**).

FRET experiments with MANT-nucleotides. In FRET experiments, 2'MANT-3'd-ATP, 3'MANT-2'd-ATP and MANT-ATP (300 nM final concentration each) were added first to the buffer, and autofluorescence of MANT-nucleotides due to excitation at 280 nm was detected at 450 nm (dotted line, Fig. **1**). When CyaA was added,

Molecular Pharmacology Fast Forward. Published on June 6, 2007 as DOI: 10.1124/mol.107.034413
This article has not been copyedited and formatted. The final version may differ from this version.

tryptophan and tyrosine fluorescence occurred at 350 nm (solid line). Upon addition of CaM, FRET (decrease in emission at 350 nm and increase in emission at 430 nm) occurred for 2´MANT-3´d-ATP and 3´MANT-2´d-ATP (Figs. **1A** and **1B**, dashed lines), but not for MANT-ATP (Fig. **1C**), MANT-GTP, MANT-ITP, MANT-CTP and MANT-UTP (data not shown). When FRET experiments were performed using the tryptophan-specific excitation wavelength of 295 nm (Lakowicz, 1999), fluorescence intensity at 350 nm decreased 3-4-fold. The relative magnitude of FRET with 2'MANT-3'd-ATP and 3'MANT-2'd-ATP remained unchanged upon tryptophan-selective excitation (data not shown). Thus, FRET resulted from excitation of W69 and W242 and tyrosine residues. Y75, Y122, Y263, Y333, Y345 and Y350 are located in a distance of less than 20 Å from the catalytic site. Thus, in order to obtain high FRET signals, it is favorable to excite both tyrosine and tryptophan residues.

PMEApp (**1**) inhibited FRET in a concentration-dependent manner (Fig. **2**). Half-maximal displacement of 300 nM 3´MANT-2´d-ATP occurred at a PMEApp concentration of about 50 nM, which is compatible with the notion that PMEApp is a much more potent CyaA inhibitor than 3´MANT-2´d-ATP (Table **1**). Kinetics of CyaA FRET stimulation by CaM and inhibition by PMEApp occurred within mixing time (few seconds). These data show that FRET was specific and reversible.

By determining FRET with MANT-nucleotides at increasing concentrations after addition of CaM, saturation curves were obtained (Fig. **3**). Apparent K_d values were 400 nM for 2´MANT-3´d-ATP (**A**) and 300 nM for 3´MANT-2´d-ATP (**B**). For MANT-ATP, MANT-GTP, MANT-ITP, MANT-CTP and MANT-UTP, K_d values could not be determined due to absent or minimal FRET (data not shown). Thus, MANT isomerization may impede with energy capture of the fluorophore from tryptophan and tyrosine residues.

Molecular Pharmacology Fast Forward. Published on June 6, 2007 as DOI: 10.1124/mol.107.034413
This article has not been copyedited and formatted. The final version may differ from this version.

We used CyaA at a final concentration of just 300 nM in an assay volume of 70 µL in FRET studies, corresponding to 0.8 µg of CyaA for one measurement. As the consumption of protein is low, as the production of CyaA can be accomplished at large scale (Shen et al., 2002) and as kinetics occur within seconds (Fig. **2**), fluorimetric high-throughput screening of potential novel inhibitors is feasible, avoiding the use of radioactive AC assays. Since fluorescent nucleotides (e. g. 3´MANT-2´d-ATP) were competitively displaced from CyaA by PMEApp (Fig. **2**), the affinity of non-labeled inhibitors may also be estimated using this approach. In saturation experiments (Fig. **3**), apparent K_d values were estimated to be 400 nM for 2´MANT-3´d-ATP (**A**) and 300 nM for 3´MANT-2´d-ATP (**B**). The results from FRET experiments are in good agreement with the corresponding K_i-values determined in the AC activity assay (Table **1**).

Direct fluorescence experiments with MANT-nucleotides. Nucleotides were excited at 350 nm and emission was scanned from 380 nm to 550 nm. Addition of CyaA to cuvettes containing 2'MANT-3'd-ATP or 3'MANT-2'd-ATP did not increase their intrinsic fluorescence (Figs. **4A** and **4B**). However, upon addition of CaM, fluorescence increased by 120% and 130%, respectively. Moreover, the emission maximum of 2'MANT-3'd-ATP and 3'MANT-2'd-ATP showed a shift to shorter wavelengths (blue shift). Under these conditions, MANT-ATP fluorescence increased only by about 40% (data not shown). For comparison, direct fluorescence of nucleotides was determined in a polar environment (water) and a hydrophobic environment (30% (v/v) dimethyl sulfoxide). Fluorescence of 100 nM 3´MANT-2´d-ATP increased by 160% when exposed to dimethyl sulfoxide (Fig. **4C**). Additionally, the emission maximum shifted to shorter wavelengths. Thus, binding of MANT-

Molecular Pharmacology Fast Forward. Published on June 6, 2007 as DOI: 10.1124/mol.107.034413
This article has not been copyedited and formatted. The final version may differ from this version.

nucleotides to CyaA transferred the MANT-group into a hydrophobic environment, probably facilitating interaction with F306 (Guo et al., 2005).

Fluorescence experiments with TNP-nucleotides. When excited at a wavelength of 405 nm, TNP-ATP, TNP-GTP, TNP-CTP and TNP-UTP showed a fluorescence peak at ~550 nm (Fig. **5**) The addition of CyaA to cuvettes containing TNP-nucleotides increased fluorescence 3-5-fold, with TNP-ATP and TNP-GTP showing the largest increases (Fig. **5A** and **5B**). The fluorescence increases with TNP-nucleotides were virtually instantaneous following CyaA addition (data not shown), indicative for rapid nucleotide/protein interaction. Moreover, we observed a blue-shift of the emission maximum of TNP-nucleotides to ~540 nm. These data indicate that binding of TNP-nucleotides to CyaA transfers the TNP-group into a hydrophobic environment. Furthermore, and in striking contrast to the results obtained with MANT-nucleotides (Figs. **2**-**4**), addition of CaM to CyaA reduced TNP-nucleotide fluorescence. This reduction in fluorescence was dependent on the specific nucleotide studied, TNP-ATP showing the smallest relative reduction (Fig. **5A**) and TNP-CTP and TNP-UTP showing the largest relative reductions (Figs. **5C** and **5D**).

Modelling of the binding modes of MANT- and TNP-nucleotides to CyaA. The crystal structure of CyaA in complex with CaM and PMEApp (Guo et al., 2005) offered us the possibility to predict the binding mode of MANT- and TNP-nucleotides. The AC domain of CyaA contains the catalytic site at the interface of two structural domains, C_A (M1 – G61, A187 – A364) and C_B (V62 – T186). Compared to PMEApp, the substrate ATP and the fluorescent nucleotides are conformationally restricted due to the semirigid ribosyl moiety. However, the spacious cavity between C_A and C_B may

Molecular Pharmacology Fast Forward. Published on June 6, 2007 as DOI: 10.1124/mol.107.034413
This article has not been copyedited and formatted. The final version may differ from this version.

accomodate the different scaffolds so that an alignment of the adenine base and the terminal phosphates is possible (Fig. **6A**). It becomes obvious that hydrophobic interactions, especially of the lipophilic edge of the desoxyribosyl moiety with L60 and of the 3'MANT group with F306, significantly contribute to the binding of 3'MANT-2'd-ATP (**21**) to CyaA (Table **1** and Fig. **3B**). In fact, non-substituted NTPs exhibited 5-170-fold lower affinities than their MANT-substituted analogs (e. g. ITP vs. MANT-ITP), and CyaA-F306A failed to increase the fluorescence signal of 3´ANT-2´d-ATP (Guo et al., 2005).

However, the question arises why PMEApp (**1**) is four orders of magnitude more potent at inhibiting CyaA than the natural and γS-substituted NTPs (**2**-**7**) if the alignment indicates similar interactions. First of all, a reasonable superposition of the phosphates and the adenine bases as shown in Fig. **6A** is only possible if the conformation of the nucleotide moiety retains a certain strain of about 3 kcal mol^{-1}. A complete minimization would displace the adenine base and, in particular, the phosphate groups from their optimal positions. Therefore, the "true" fit must be a balance between conformational strain and binding energy. Secondly, the ethoxy oxygen of PMEApp strongly interacts with E301 and N304 via a water molecule, and the ethylene bridge is also in close contact with the edge of F306.

Fig. **6B** represents the docking of 3'MANT-2'd-ATP (**21**) into CyaA in more detail. The desoxyribosyl ring adopts a 3'-exo conformation like the ribosyl moiety of MANT-ATP in complex with mammalian AC (Mou et al., 2006). The three Mg^{2+} ions are in similar positions as in the CyaA-PMEApp complex and form the same interactions. Two of them are coordinated with D188 and D190, one additionally with H298, and the third with the α- and β-phosphate. The imidazolyl-NH of H298 may be H-bonded with an oxygen of the α-phosphate. The γ-phosphate contacts the lysine

Molecular Pharmacology Fast Forward. Published on June 6, 2007 as DOI: 10.1124/mol.107.034413
This article has not been copyedited and formatted. The final version may differ from this version.

residues K65 and K58 (O-N distances ~2.8 Å). These interactions account for the higher inhibitory potencies of the triphosphates compared to the diphosphate and monophosphate analogs in Table **1**.

The adenine moiety is sandwiched between the side chains of H298 and N304 whose amide NH_2 group may form an additional H bond with the desoxyribosyl ring oxygen. The 6-amino substituent is in proximity to the backbone oxygens of V271, G299 and T300. However, the loop between G299 and N304 may align all of the nucleobases in similar position. In the case of GTP, ITP, UTP and their MANT- and TNP-derivatives, backbone NH functions of, e.g., G299 and V271 could serve as hydrogen donors for the carbonyl oxygens in 6 and 4 position, respectively. This diversity of possible interactions may account for the relatively small and inconsistent potency differences when comparing the impact of base substitution in different subsets of nucleotides, i.e. natural NTPs, MANT-NTPs, MANT-NDPs and TNP-NTPs (see Table **1**). In addition, the affinity of each nucleotide may be affected by a specific arrangement of water molecules which cannot be simply transferred from the PMEApp-bound CyaA structure.

Fig. **6B** also shows that the high potency of 3'MANT-2'd-ATP (**21**) is particularly due to ideal stacking of the phenyl rings of the inhibitor and F306. This stacking also accounts for the efficient FRET and direct fluorescence observed with 3'MANT-2'd-ATP (Figs. **1-4**). The axial position of the hydrogen atom corresponding to the 2'-OH group in 3'MANT-ATP suggests that even the 2',3'di-MANT-ATP derivative will be similarly potent since the 2'-MANT moiety may fit into a hydrophobic site consisting of P305 and F261.

This site would also be occupied by the 2'-MANT group in 2´MANT-3´d-ATP (**22**) if the desoxyribosyl ring adopts a 3'-exo conformation. However, similar

Molecular Pharmacology Fast Forward. Published on June 6, 2007 as DOI: 10.1124/mol.107.034413
This article has not been copyedited and formatted. The final version may differ from this version.

potencies of the positional isomers **21** and **22** in the AC assay (Table **1**) and fluorescence assay (Fig. **3**) as well as similar magnitudes of FRET and direct fluorescence (Figs. **1** and **4**) rather indicate analoguous interactions between the MANT-group and F306 in the complexes of CyaA with 2´MANT-3´d-ATP and 3'MANT-3'd-ATP, respectively. Fig. **6C** illustrates that docking of 2´MANT-3´d-ATP may indeed reproduce the interaction pattern of 3´MANT-2´d-ATP with CyaA shown in Fig. **6B**. The only difference is a 3'-endo conformation of the desoxyribosyl moiety as is present, e.g., in A-DNA.

Fig. **5D** shows the predicted binding mode of TNP-ATP (**26**) which is similarly potent as the isomerizing MANT-ATP derivative **8**. Despite the rigidity of the tricyclic TNP-ATP scaffold containing a spiro junction, a sufficient alignment with 3´MANT-2´d-ATP is possible so that the phosphate groups, the adenine base, and the phenyl moieties may interact with the same CyaA sites. This superposition implies a relatively deep position of TNP-ATP in the cavity. The interaction of F306 with the TNP group is weaker than with MANT (no optimal position, lower hydrophobicity). However, hydrogen bonds of two ribosyl oxygens with the side chains of H298 and N304, respectively, may in part counterbalance reduced hydrophobic interactions and higher conformational strain. In addition, the intrinsic fluorescence properties of TNP-nucleotides, i.e. higher fluorescence increases upon transfer into a hydrophobic environment than with MANT-nucleotides (Jameson and Eccleston, 1997; Hiratsuka, 2003), more than compensate for the suboptimal positioning of the TNP-group relative to F306, allowing for the detection of larger fluorescence increases than with MANT-nucleotides (Figs. **4** and **5**). Interestingly, the inhibitory potency of TNP derivatives **26-29** is more dependent on the specific nucleobase than in the corresponding subseries of MANT-nucleotides **8**, **10**, **14** and **15** and the unsubstituted NTPs, ATP, GTP (**2**), CTP (**5**) and UTP (**6**). Probably, the rigid scaffold

Molecular Pharmacology Fast Forward. Published on June 6, 2007 as DOI: 10.1124/mol.107.034413
This article has not been copyedited and formatted. The final version may differ from this version.

of the TNP-nucleotides does not enable an optimal fit of guanine and the pyrimidines to the backbone of the loop between G299 and N304

The lower substrate K_m and V_{max} values as well as the generally 5-40 fold higher potency of the inhibitors under Mn^{2+} conditions than under Mg^{2+} conditions clearly point to considerably tighter binding with the former cation. This increase in the free energy of binding of up to ~2 kcal mol^{-1} should be mainly due to stronger Mn^{2+}-phosphate binding. No further conclusions can be drawn from the docking approaches based on force field methods and without a CyaA crystal structure with Mn^{2+} instead of Mg^{2+}.

Molecular Pharmacology Fast Forward. Published on June 6, 2007 as DOI: 10.1124/mol.107.034413
This article has not been copyedited and formatted. The final version may differ from this version.

Discussion

Spacious catalytic site of CyaA. The catalytic site of CyaA forms a large cavity with substantial conformational freedom to accommodate structurally diverse ligands. Specifically, not only adenine nucleotides, but also other purine and even pyrimidine nucleotides reduce the catalytic activity of CyaA (Table **1**) due to flexible fit to the backbone of the loop between G299 and N304 (Fig. **6**). Effective interaction of CyaA with purine and pyrimidine nucleotides is also clearly documented in the fluorescence experiments with TNP-ATP, TNP-GTP, TNP-CTP and TNP-UTP (Fig. **5**), monitoring interaction of the TNP-group with F306 (Fig. **6D**). The distinct fluorescence responses upon interaction of CyaA with various TNP-nucleotides in the absence and presence of CaM are indicative for slightly different orientations of TNP-nucleotides in the catalytic site of CyaA. Moreover, various MANT-nucleotides (**12**-**15**) exhibiting higher affinity for CyaA than TNP-nucleotides (Table **1**) did not give rise to FRET with CyaA. These findings suggest that differences in affinity do not account for the different fluorescence responses with various nucleotides. Rather, the differences in fluorescence properties point to differences in orientation of the nucleotides in the catalytic site. Taken together, all those findings are in accordance with the modeling data and support the notion of a spacious catalytic site of CyaA.

Towards the development of selective CyaA inhibitors. As the inhibitory profile of CyaA differs considerably from that of mammalian ACs (Gille et al., 2004; Mou et al., 2005, 2006), development of more potent and selective CyaA inhibitors is feasible. For all inhibitors studied, the TNP substituent was substantially less effective in increasing nucleotide affinity than MANT/ANT. While ANT-ATP was more potent than MANT-ATP, the MANT-group was superior to ANT in case of MANT-GTP vs.

Molecular Pharmacology Fast Forward. Published on June 6, 2007 as DOI: 10.1124/mol.107.034413
This article has not been copyedited and formatted. The final version may differ from this version.

ANT-GTP. The additional methyl group in MANT compared to ANT may reduce mobility of the fluorescent group and, thereby, facilitate alignment with F306, depending on the specific nucleobase present.

For all MANT-NDP/NTP pairs studied so far, elimination of the γ-phosphate group substantially decreased inhibitor affinity. As an example, MANT-IDP (**18**) was almost 20-fold less potent than MANT-ITP (**12**), and the omission of the β-phosphate in MANT-IMP (**30**) further reduced affinity compared to MANT-IDP. The importance of the polyphosphate chain for effective interaction of nucleotides with the catalytic site is also supported by our modeling data (Fig. **6B**). For future applications of MANT-nucleotides in intact-cell assays, nucleotides with a phosphate tail resistant to hydrolysis are needed (Rottlaender et al., 2007). As the potency of γS-substituted MANT-nucleotides was higher in case of MANT-ATPγS vs. MANT-ATP and MANT-GTPγS vs. MANT-GTP, the design of potent nucleotides resistant to hydrolysis is feasible.

An unexpected side product in our synthesis scheme of MANT-ITP (**12**) was di-MANT-IMP (**31**). Even more unexpectedly, addition of a second MANT-group to the ribosyl ring in di-MANT-IMP (**31**) caused an increase in affinity as compared to MANT-IMP (**30**) under Mn^{2+} and Mg^{2+} conditions (Table **1**) which may be attributed to interactions of the 2'MANT-group with a hydrophobic site consisting of F305 and F261 (Fig. **6B**). Thus, the introduction of a second MANT/ANT-group or other bulky substituents should be considered in future inhibitor design projects in order to increase inhibitor affinity. In addition, given the surprising differences in fluorescence responses between MANT- and TNP-nucleotides, di-MANT-nucleotides may provide valuable conformational probes to better understand the mechanisms of CyaA activation.

Molecular Pharmacology Fast Forward. Published on June 6, 2007 as DOI: 10.1124/mol.107.034413
This article has not been copyedited and formatted. The final version may differ from this version.

Considering the bases, hypoxanthine is superior to other purine and pyrimidine bases (Table **1**). Moreover, 2´MANT-3´d-ATP and 3´MANT-2´d-ATP are considerably more potent than MANT-ATP. Therefore, 2´MANT-3´d-ITP and 3´MANT-2´d-ITP are interesting future candidates as potential novel CyaA inhibitors. Further increase in potency and selectivity of PMEApp may be achieved by changing the adenine base to hypoxanthine and by introducing a MANT/ANT substituent.

Like CyaA, *Bacillus anthracis* AC toxin edema factor also bears a phenylalanine residue close to the catalytic site (Guo et al., 2005). Structural comparison of CyaA with edema factor revealed that F306 of CyaA is the analog of F586 in edema factor, forming hydrophobic interactions with the MANT-group, thus increasing direct fluorescence of MANT-nucleotides. The inhibitory profile of edema factor differs considerably from that of CyaA. Specifically, MANT-ATP inhibits catalytic activity of CyaA with almost 25-fold lower potency than catalysis by edema factor (Gille et al., 2004). In case of 3´MANT-2´d-GTP, 3´MANT-2´d-ATP and MANT-ADP, the decreases in potency of CyaA inhibition compared to edema factor inhibition were 22-fold, 25-fold and 40-fold, respectively. Based on these differences in enzymological properties, it is also reasonable to assume that the fluorescence analysis of edema factor with MANT- and TNP-nucleotides will give very different results than with CyaA.

We have solved the crystal structure of mammalian C1:C2 AC in complex with MANT-GTP, MANT-ATP and TNP-ATP (Mou et al., 2005, 2006). Based on crystallographic studies, we have developed a tripartite model for mammalian AC with a binding site for the base, the ribosyl substituent and the phosphate tail (Mou et al., 2005, 2006). In this model, the base site possesses the smallest influence, whereas the ribosyl substituent has a strong impact. This model can also be applied to CyaA (Fig. **6)**. Specifically, a variety of purine and pyrimidine nucleotides inhibit

Molecular Pharmacology Fast Forward. Published on June 6, 2007 as DOI: 10.1124/mol.107.034413
This article has not been copyedited and formatted. The final version may differ from this version.

CyaA, suggesting that the base does not greatly determine the potency of 2´,3´-ribosyl substituted inhibitors. In contrast, introduction of a MANT/ANT-group increased inhibitor potency at CyaA up to 170-fold (e. g. ITP vs. MANT-ITP), pointing to the critical importance of the ribosyl substituent. However, TNP substitution showed a much smaller effect on inhibitor affinity for CyaA than for C1:C2 (Mou et al., 2006) (Table **1**), highlighting the substantial structural differences between the binding. Specifically, mammalian AC possesses a large hydrophobic pocket consisting of several amino acids accommodating the 2',3'-ribosyl substituent (Mou et al., 2005, 2006), whereas in case of CyaA, just one amino acid, namely F306, participates in hydrophobic interactions with MANT- and TNP-nucleotides (Fig. **6**).

The role of divalent cations. It is also important to emphasize that in future studies, inhibitors should be studied both under Mg^{2+}- and Mn^{2+}-conditions as there are differences in the rank order of potency of compounds under those conditions. Moreover, exchange of Mn^{2+} against Mg^{2+} increases V_{max} but decreases K_m (Table **1**). Crystallographic studies are required to understand those substantial differences between Mn^{2+} and Mg^{2+}. It is reasonable to assume that under physiological conditions, Mg^{2+} rather than Mn^{2+} is relevant. Probably, Mn^{2+} is only an (important) experimental tool to facilitate molecular analysis of CyaA. Specifically, in the presence of Mg^{2+}, detection of significant increases in FRET and direct fluorescence with MANT-nucleotides was impossible (data not shown).

CaM-independent interaction of CyaA with nucleotides. The fact that fluorescence of TNP-nucleotides increased upon interaction with CyaA in the absence of the activator CaM (Fig. **5**) indicates that the nucleotide-binding site of CyaA is already functional in the catalytically inactive toxin. However, our data

Molecular Pharmacology Fast Forward. Published on June 6, 2007 as DOI: 10.1124/mol.107.034413
This article has not been copyedited and formatted. The final version may differ from this version.

suggest that CyaA does not bind MANT-nucleotides in the absence of CaM, since FRET and direct fluorescence with MANT-nucleotides was completely dependent on CaM (Figs. **1-4**). In contrast to CyaA, mammalian C1:C2 does bind MANT-nucleotides, to some extent, in the absence of the activator forskolin (Mou et al., 2005, 2006), again supporting the concept of substantial structural differences between mammalian and bacterial AC. These data also imply that binding of CaM to CyaA induces a conformational change in the toxin that allows MANT-nucleotides to bind. The identification of the precise nature of this conformational change requires crystallization of CyaA complexes with TNP-nucleotides in the absence and presence of CaM as well as of CyA with MANT-nucleotides in the presence of CaM. The opposite fluorescence responses of TNP-nucleotides and MANT-nucleotides to CaM are in agreement with the modeling studies showing that the TNP- and MANT-group adopt similar but not identical positions in the catalytic site of CyaA (Fig. **6D**). The dramatic differences in fluorescence responses of TNP- and MANT-nucleotides in the absence and presence of CaM also demonstrate that these nucleotides are extremely sensitive probes for detecting small differences in nucleotide/CyaA interactions.

Another implication of the CaM-independent binding of TNP-nucleotides to CyaA is that the catalytic site of CyaA possesses different binding properties than the site in the presence of CaM, offering additional possibilities for inhibitor design and increasing inhibitor-selectivity. Comparison of inhibition profiles of non-fluorescent nucleotides on TNP-nucleotide fluorescence bound to CyaA in the absence and presence of CaM is a feasible approach. With respect to catalysis, such comparison is impossible because enzymatic activity obligatorily depends on CaM (Ladant and Ullmann, 1999; Shen et al., 2002).

Molecular Pharmacology Fast Forward. Published on June 6, 2007 as DOI: 10.1124/mol.107.034413
This article has not been copyedited and formatted. The final version may differ from this version.

Conclusions. In the present study we have shown that the catalytic site of CyaA possesses unique pharmacological properties compared to other mammalian and bacterial ACs. The spacious catalytic site of CyaA accommodates a broad variety of 2',3'-substituted nucleotides, even di-MANT-nucleotides. Some inhibitors can bind to CyaA even in the absence of CaM, and there is evidence for distinct interaction of CyaA with MANT-nucleotides and TNP-nucleotides. Finally, the fluorescence assays described in this study can be used for identification of novel CyaA inhibitors, ultimately resulting in the development of novel drugs for prophylaxis of whooping cough.

Acknowledgments

We thank Mrs. Susanne Brüggemann and Mrs. Astrid Seefeld for expert technical assistance. Thanks are also due to the Reviewers of this paper for their constructive critique. This paper is dedicated to Günter Schultz, who made seminal contributions to our understanding of adenylyl cyclases, on the occasion of his 70th birthday.

Molecular Pharmacology Fast Forward. Published on June 6, 2007 as DOI: 10.1124/mol.107.034413
This article has not been copyedited and formatted. The final version may differ from this version.

References

Ahuja N, Kumar P and Bhatnagar R (2004) The adenylate cyclase toxins. *Crit Rev Microbiol* **30**:187-196.

Boyd AP, Ross PJ, Conroy H, Mahon N, Lavelle EC and Mills KH (2005) *Bordetella pertussis* adenylate cyclase toxin modulates innate and adaptive immune responses: distinct roles for acylation and enzymatic activity in immunomodulation and cell death. *J Immunol* **175**:730-738.

Carbonetti NH, Artamonova GV, Andreasen C and Bushar N (2005) *Pertussis* toxin and adenylate cyclase toxin provide a one-two punch for establishment of *Bordetella pertussis* infection of the respiratory tract. *Infect Immun* **73**:2698-2703.

Clark M, Cramer R.D. III and Van Opdenbosch N (1989) Validation of the general purpose Tripos 5.2 force field. *J Comp Chem* **10**:982-1012.

Confer DL and Eaton JW (1982) Phagocyte impotence caused by an invasive bacterial adenylate cyclase. *Science* **217**:948-950.

Cornell WD, Cieplak P, Bayly CI, Gould IR, Merz KMJ, Ferguson DM, Spellmeyer DC, Fox T, Caldwell JW and Kollman PA (1995) A second generation force field for the simulation of proteins and nucleic acids. *J Am Chem* **117**:5179-5197.

Ghose AK, Viswanadhan VN and Wendoloski JJ (1998) Prediction of hydrophobic (lipophilic) properties of small organic molecules using fragmental methods: an analysis of ALOGP and CLOGP methods. *J Phys Chem* **102**:3762-3772.

Gille A, Lushington GH, Mou TC, Doughty MB, Johnson RA and Seifert R (2004) Differential inhibition of adenylyl cyclase isoforms and soluble guanylyl cyclase by purine and pyrimidine nucleotides. *J Biol Chem* **279**:19955-19969.

Gille A and Seifert R (2003) 2'(3')-*O*-(*N*-methylanthraniloyl)-substituted GTP analogs: a novel class of potent competitive adenylyl cyclase inhibitors. *J Biol Chem* **278**:12672-12679.

Gilles AM, Munier H, Rose T, Glaser P, Krin E, Danchin A, Pellecuer C and Barzu O (1990) Intrinsic fluorescence of a truncated *Bordetella pertussis* adenylate cyclase expressed in *Escherichia coli*. *Biochemistry* **29**:8126-8130.

Guo Q, Shen Y, Lee YS, Gibbs CS, Mrksich M and Tang WJ (2005) Structural basis for the interaction of *Bordetella pertussis* adenylyl cyclase toxin with calmodulin. *EMBO J* **24**:3190-3201.

Heiden W, Moeckel G and Brickmann J (1993) A new approach to analysis and display of local lipophilicity/hydrophilicity mapped on molecular surfaces. *J Comput Aided Mol Des* **7**:503-514.

Hewlett EL, Donato GM and Gray MC (2006) Macrophage cytotoxicity produced by adenylate cyclase toxin from *Bordetella pertussis*: more than just making cyclic AMP! *Mol Microbiol* **59**:447-459.

Hewlett EL, Gordon VM, McCaffery JD, Sutherland WM and Gray MC (1989) Adenylate cyclase toxin from *Bordetella pertussis*. Identification and purification of the holotoxin molecule. *J Biol Chem* **264**:19379-19384.

Hiratsuka T (1983) New ribose-modified fluorescent analogs of adenine and guanine nucleotides available as substrates for various enzymes. *Biochim Biophys Acta* **742**:496-508.

Hiratsuka T (2003) Fluorescent and colored trinitrophenylated analogs of ATP and GTP. *Eur J Biochem* **270**:3479-3485.

Jameson DM and Eccleston JF (1997) Fluorescent nucleotide analogs: synthesis and applications. *Methods Enzymol* **278**:363-390.

Johnson RA and Shoshani I (1990) Inhibition of *Bordetella pertussis* and *Bacillus anthracis* adenylyl cyclases by polyadenylate and "P"-site agonists. *J Biol Chem* **265**:19035-19039.

Ladant D and Ullmann A (1999) *Bordatella pertussis* adenylate cyclase: a toxin with multiple talents. *Trends Microbiol* **7**:172-176.

Lakowicz JR (1999) *Principles of fluorescence spectroscopy*. Kluwer Academic/Plenum, New York.

Mock M and Ullmann A (1993) Calmodulin-activated bacterial adenylate cyclases as virulence factors. *Trends Microbiol* **1**:187-192.

Mou TC, Gille A, Fancy DA, Seifert R and Sprang SR (2005) Structural basis for the inhibition of mammalian membrane adenylyl cyclase by 2 '(3')-*O*-(*N*-methylanthraniloyl)-guanosine 5'-triphosphate. *J Biol Chem* **280**:7253-7261.

Mou TC, Gille A, Suryanarayana S, Richter M, Seifert R and Sprang SR (2006) Broad specificity of mammalian adenylyl cyclase for interaction with 2',3'-substituted purine- and pyrimidine nucleotide inhibitors. *Mol Pharmacol* **70**:878-886.

Rottlaender D, Matthes J, Vatner SF, Seifert R and Herzig S (2007) Functional adenylyl cyclase inhibition in murine cardiomyocytes by 2'(3')-*O*-(*N*-methylanthraniloyl)-guanosine 5'-[γ-thio]triphosphate. *J Pharmacol Exp Ther* **321**:608-615.

Sarfati RS, Kansal VK, Munier H, Glaser P, Gilles AM, Labruyere E, Mock M, Danchin A and Barzu O (1990) Binding of 3'-anthraniloyl-2'-deoxy-ATP to calmodulin-activated adenylate cyclase from *Bordetella pertussis* and *Bacillus anthracis*. *J Biol Chem* **265**:18902-18906.

Shen Y, Lee YS, Soelaiman S, Bergson P, Lu D, Chen A, Beckingham K, Grabarek Z, Mrksich M and Tang WJ (2002) Physiological calcium concentrations regulate calmodulin binding and catalysis of adenylyl cyclase exotoxins. *EMBO J* **21**:6721-6732.

Shen Y, Zhukovskaya NL, Zimmer MI, Soelaiman S, Bergson P, Wang CR, Gibbs CS and Tang WJ (2004) Selective inhibition of anthrax edema factor by adefovir, a drug for chronic hepatitis B virus infection. *Proc Natl Acad Sci USA* **101**:3242-3247.

Soelaiman S, Wei BQ, Bergson P, Lee YS, Shen Y, Mrksich M, Shoichet BK and Tang WJ (2003) Structure-based inhibitor discovery against adenylyl cyclase toxins from pathogenic bacteria that cause anthrax and whooping cough. *J Biol Chem* **278**:25990-25997.

Molecular Pharmacology Fast Forward. Published on June 6, 2007 as DOI: 10.1124/mol.107.034413
This article has not been copyedited and formatted. The final version may differ from this version.

Footnotes

[†]Supported by the Deutsche Forschungsgemeinschaft (Graduiertenkolleg 760 "Medicinal Chemistry: Molecular Recognition - Ligand-Receptor Interactions" and research grant Se 529/5-1 to R.S.). P.S. was supported by the “Research Internships in Science and Engineering (RISE) programme” of the German Academic Exchange service (DAAD).

[1]Send reprint requests to:

Dr. Roland Seifert

Department of Pharmacology and Toxicology, Institute of Pharmacy,

University of Regensburg

Universitaetsstr. 31

D-93053 Regensburg, Germany

Telephone: +49-941-943-4770. Fax: +49-941-943-4772.

E-mail: roland.seifert@chemie.uni-regensburg.de

Molecular Pharmacology Fast Forward. Published on June 6, 2007 as DOI: 10.1124/mol.107.034413
This article has not been copyedited and formatted. The final version may differ from this version.

Figure legends

Figure 1: Monitoring of MANT-nucleotide binding to the catalytic site of CyaA using FRET. The assay buffer consisted of 75 mM HEPES/NaOH, 100 µM $CaCl_2$, 100 mM KCl and 5 mM $MnCl_2$, pH 7.4. Nucleotides (**A**: 2´MANT-3´d-ATP, **B**: 3´MANT-2´d-ATP, **C**: MANT-ATP) were added to the buffer to yield 300 nM final concentration, and emission was scanned at an excitation wavelength of 280 nm. CyaA protein and calmodulin were added successively to yield 300 nM final concentration. Shown are superimposed recordings of a representative experiment. Similar data were obtained in 3 independent experiments. a.u., arbitrary unit.

Figure 2: Time-resolved activation of CyaA by CaM and stepwise abolishment of FRET by PMEApp. Excitation wavelength was 280 nm and emission was detected at 430 nm over time. Successively, 300 nM 3´MANT-2´d-ATP (**1**), 300 nM CyaA protein (**2**), 300 nM CaM (**3**) and PMEApp in the given final concentrations (addition steps **4**, 10 nM; **5**, 30 nM; **6**, 70 nM; **7**, 1.6 µM) were added. A recording of a representative experiment is shown. Similar data were obtained in 4 independent experiments. a.u., arbitrary unit.

Figure 3: Saturation curves of 2´MANT-3´d-ATP and 3´MANT-2´d-ATP binding to activated CyaA. Each data point was determined in an independent experiment as described in “Materials and Methods”. Final concentrations of CyaA and CaM were 300 nM each. The fluorescence increase at 430 nm was calculated by subtracting the fluorescence at 430 nm after addition of CyaA from the maximal fluorescence at 430 nm after addition of CyaA/CaM. Data were analyzed by non-linear regression using the Prism 4.02 software. Similar data were obtained in 3 independent experiments. a.u., arbitrary unit.

Figure 4: Direct fluorescence of MANT-nucleotides. The excitation wavelength was 350 nm, and emission was scanned from 380 nm to 550 nm. Successively, 100 nM nucleotide, 2.4 µM CyaA and 2.4 µM CaM were added to the cuvette (**A**) and (**B**). In order to mimic binding of the MANT-group to a hydrophobic binding pocket, 3´MANT-2´d-ATP was directly excited in water plus dimethyl sulfoxide (DMSO) 30% (v/v) (**C**). Shown are superimposed recordings of a representative experiment. Similar data were obtained in 5 independent experiments. a.u., arbitrary unit.

Figure 5: Fluorescence analysis of the interactions of TNP-nucleotides with CyaA. The excitation wavelength was 405 nm, and emission was scanned from 480 nm to 620 nm. Successively, 5 µM nucleotide, 5 µM CyaA and 5 µM CaM were added to the cuvette. **A**, TNP-ATP; **B**, TNP-GTP; **C**, TNP-CTP; **D**, TNP-UTP. Shown are superimposed recordings of a representative experiment. Similar data were obtained in 3-5 independent experiments. a.u., arbitrary unit.

Molecular Pharmacology Fast Forward. Published on June 6, 2007 as DOI: 10.1124/mol.107.034413
This article has not been copyedited and formatted. The final version may differ from this version.

Figure 6: Docking of representative MANT- and TNP-nucleotides to CyaA. The models are based on the crystal structure of CyaA in complex with PMEApp, PDB 1zot (Guo et al., 2005) (clockwise arrangement of the images for better comparability of panels B and C). Colors of atoms, unless otherwise indicated: orange – P, red – O, blue – N, white – C, H, green spheres – Mg^{2+}. **A.** Overview of the binding site, represented by the lipophilic potential mapped onto a MOLCAD Connolly surface (brown – hydrophobic areas, green and blue – polar areas). Docked ligands: PMEApp (C atoms in magenta); 3´MANT-2´d-ATP (C and H atoms in yellow). **B.** Docking of 3´MANT-2´d-ATP (**21**). Amino acids within a sphere of ~3 Å around the ligand are labeled. The protein backbone is schematically represented by a tube. C atoms of the backbone are colored in dark cyan, C atoms of the side chains in light cyan. **C.** Docking of 2´MANT-3´d-ATP (**22**). Representation of the backbone and the side chains like in panel B. For clarity, some labels are omitted (see panel B). **D.** Docking of TNP-ATP (**26**). For comparison, 3´MANT-2´d-ATP is shown in the same position like in panel B (all atoms colored in magenta). Only amino acids with suggested interactions specific for TNP-ATP are labeled. Representation of the backbone and the side chains like in panel B.

Molecular Pharmacology Fast Forward. Published on June 6, 2007 as DOI: 10.1124/mol.107.034413
This article has not been copyedited and formatted. The final version may differ from this version.

Table 1: Potencies of inhibitors at CyaA.

			Mn^{2+}	Mg^{2+}
		K_m	45 ± 6	609 ± 62
		V_{max}	165 ± 21	861 ± 106
Cpd.				
1	PMEApp		0.001 ± 0.0003	0.025 ± 0.002
2	GTP		27 ± 6	260 ± 32
3	ITP		100 ± 20	1,100 ± 220
4	ITPγS		77	ND
5	CTP		35 ± 1	270 ± 43
6	UTP		120 ± 14	330 ± 80
7	UTPγS		36	ND
8	MANT-ATP		4.3 ± 0.4	51 ± 1
9	MANT-ATPγS		1.2 ± 0.4	15 ± 2
10	MANT-GTP		5.9 ± 1.0	16 ± 2
11	MANT-GTPγS		5.4 ± 0.5	7.4 ± 0.1
12	MANT-ITP		0.6 ± 0.1	16 ± 4
13	MANT-ITPγS		1.8 ± 0.3	31 ± 2
14	MANT-CTP		1.1 ± 0.1	36 ± 4
15	MANT-UTP		2.6 ± 0.3	42 ± 9
16	MANT-ADP		12 ± 2	91 ± 16
17	MANT-GDP		60	ND
18	MANT-IDP		11 ± 3	> 100
19	MANT-CDP		18 ± 3	> 100
20	MANT-UDP		43 ± 1	> 100
21	3´MANT-2´d-ATP		0.2 ± 0.04	32 ± 7
22	2´MANT-3´d-ATP		0.3 ± 0.04	22 ± 4
23	ANT-ATP		1.3 ± 0.1	20 ± 3
24	ANT-GTP		29 ± 0.3	> 100
25	ANT-ADP		11 ± 1	> 100
26	TNP-ATP		6.5 ± 0.2	110 ± 23
27	TNP-GTP		20 ± 3	320 ± 7
28	TNP-CTP		10 ± 0.4	410 ± 9
29	TNP-UTP		58 ± 8	780 ± 38
30	MANT-IMP		> 100	> 100
31	Di-MANT-IMP		20 ± 3	37 ± 3

Molecular Pharmacology Fast Forward. Published on June 6, 2007 as DOI: 10.1124/mol.107.034413
This article has not been copyedited and formatted. The final version may differ from this version.

AC toxin activities were determined as described under “Materials and Methods”. Apparent K_m and V_{max} values were obtained by non-linear regression analysis of substrate-saturation experiments and are the means ± SEM of 3-5 independent experiments. K_m values are given in µM, V_{max} values are given as molar turnover numbers (s^{-1}). K_i-values are given in µM and are the means ± SEM of at least 3 experiments performed in duplicates. For determination of the inhibitory potencies of various purine and pyrimidine nucleotides, reaction mixtures contained 100 mM KCl, 10 µM free Ca^{2+}, 5 mM free Mn^{2+} or Mg^{2+}, 100 µM EGTA, 40 µM ATP, 0.2 µCi/tube [α–^{32}P]ATP, 100 µM cAMP, 100 nM calmodulin, 10 pM CyaA in 75 mM HEPES/NaOH, pH 7.4, and nucleotides at concentrations from 100 pM to 2 mM as appropriate to construct concentration-response curves. The K_i-value for **1** under Mg^{2+}-conditions was taken from Shen et al. (2004). The K_i-values for **4**, **7** and **17** under Mn^{2+}-conditions were taken from Gille et al. (2004). Inhibition curves were analyzed by non-linear regression using the Prism 4.02 software (Graphpad, San Diego, CA).

Cpd., compound.

Figure 1

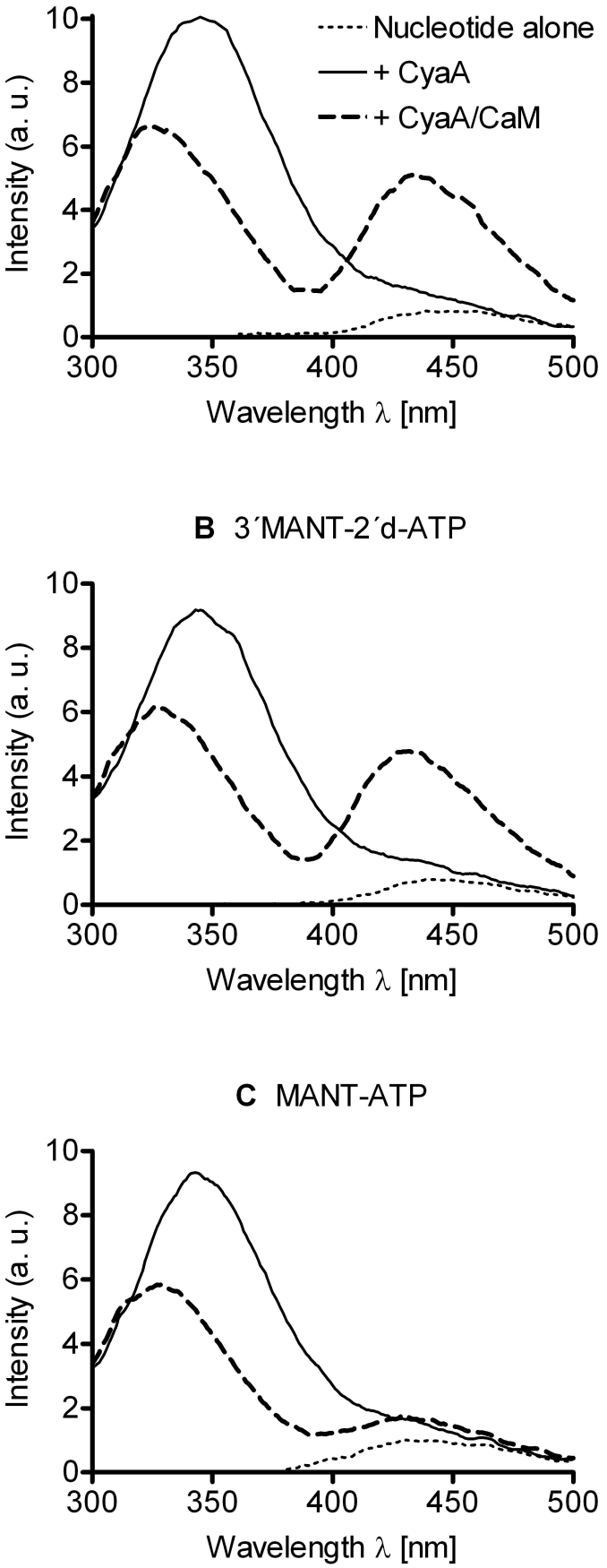
A 2´MANT-3´d-ATP
Nucleotide alone
+ CyaA
+ CyaA/CaM
Intensity (a. u.)
Wavelength λ [nm]
B 3´MANT-2´d-ATP
Intensity (a. u.)
Wavelength λ [nm]
C MANT-ATP
Intensity (a. u.)
Wavelength λ [nm]

Figure 2

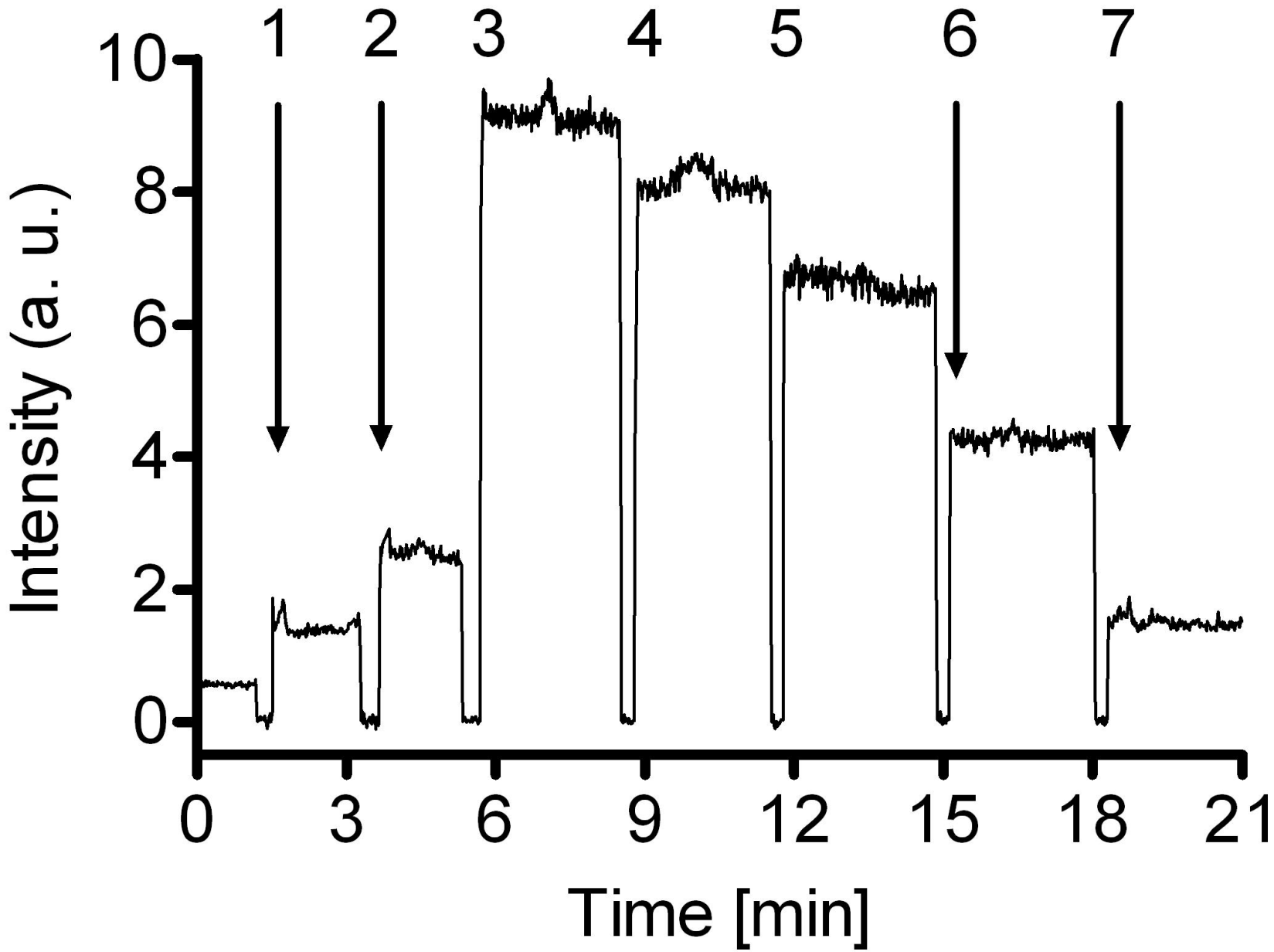

Figure 3

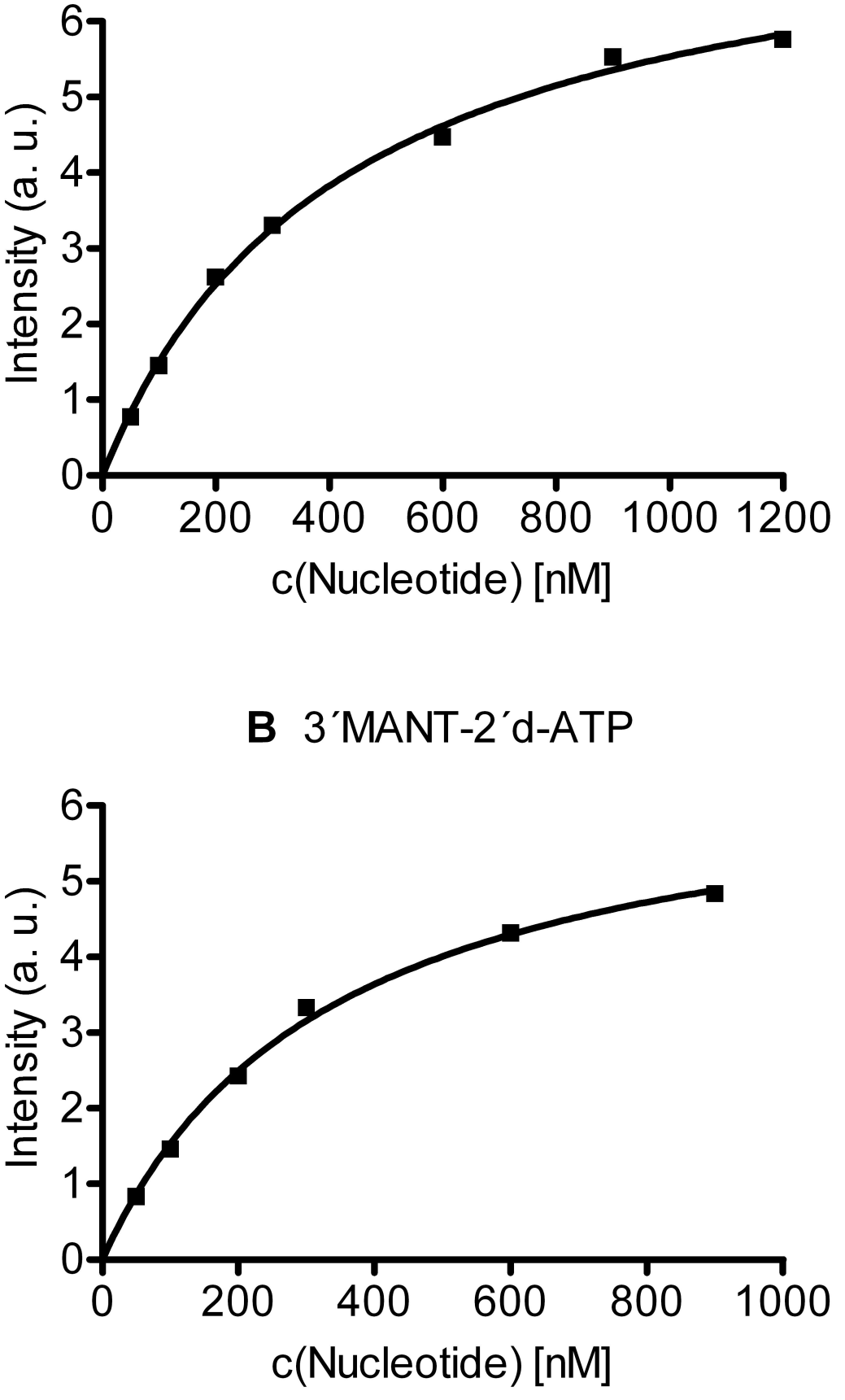
A 2´MANT-3´d-ATP
Intensity (a. u.)
0
1
2
3
4
5
6
0
200
400
600
800
1000
1200
c(Nucleotide) [nM]
B 3´MANT-2´d-ATP
Intensity (a. u.)
0
1
2
3
4
5
6
0
200
400
600
800
1000
c(Nucleotide) [nM]

Figure 4

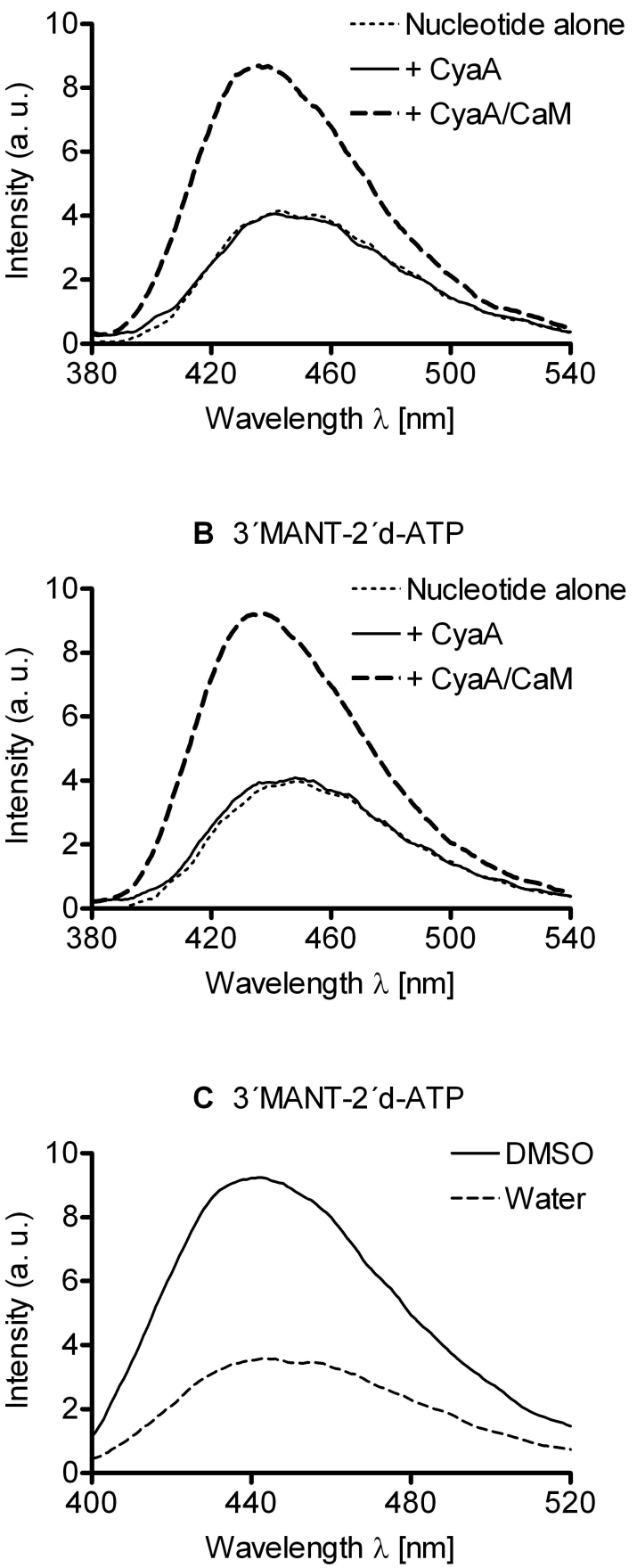
A 2'MANT-3'd-ATP
Nucleotide alone
+ CyaA
+ CyaA/CaM
Intensity (a. u.)
Wavelength λ [nm]
B 3´MANT-2´d-ATP
Nucleotide alone
+ CyaA
+ CyaA/CaM
Intensity (a. u.)
Wavelength λ [nm]
C 3´MANT-2´d-ATP
DMSO
Water
Intensity (a. u.)
Wavelength λ [nm]

Figure 5

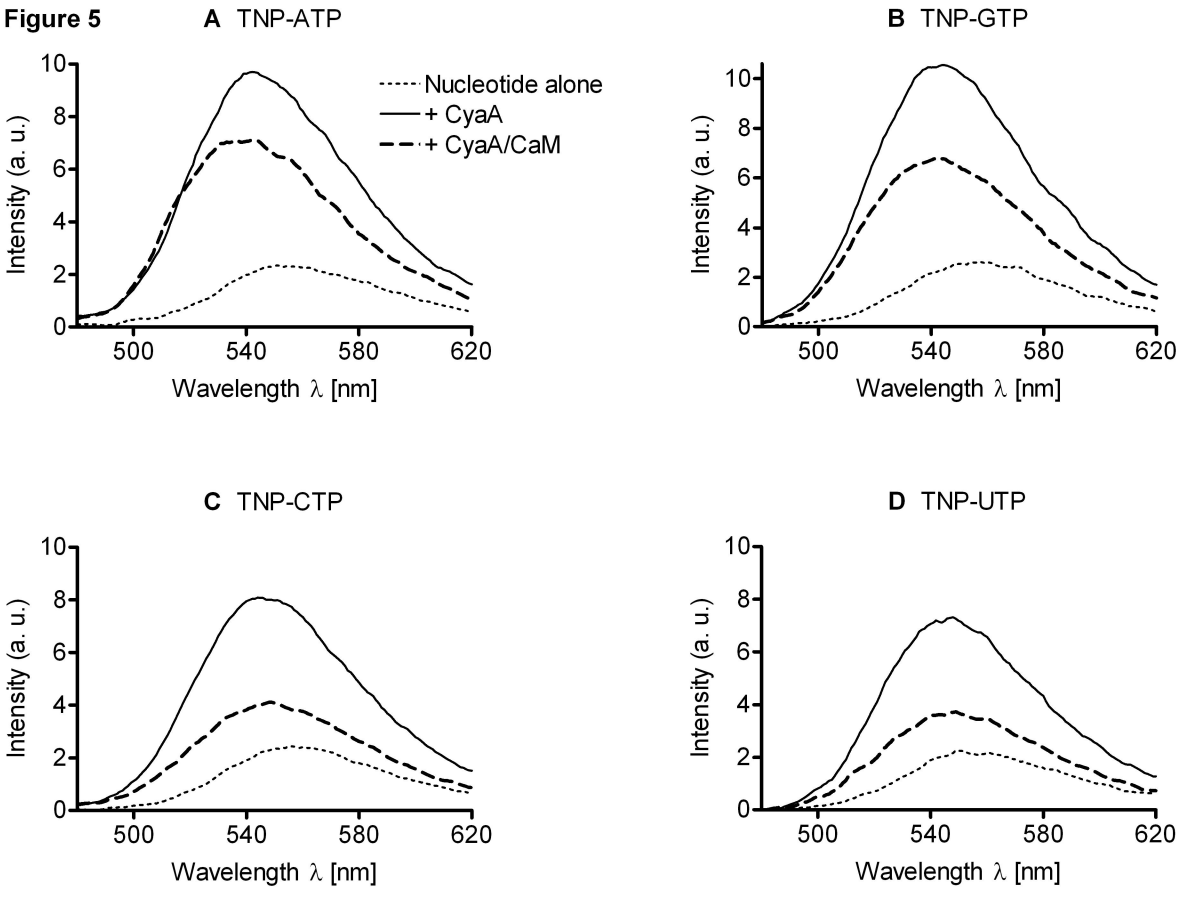
A TNP-ATP
B TNP-GTP
C TNP-CTP
D TNP-UTP
Nucleotide alone
+ CyaA
+ CyaA/CaM
Intensity (a. u.)
Wavelength λ [nm]
0
2
4
6
8
10
500
540
580
620

Figure 6

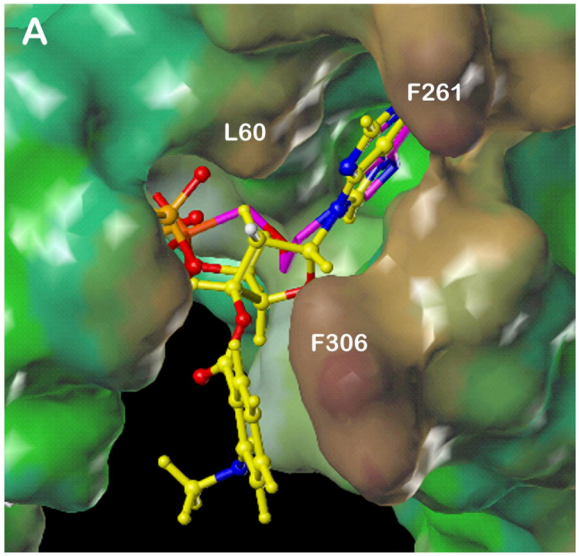
A
F261
L60
F306

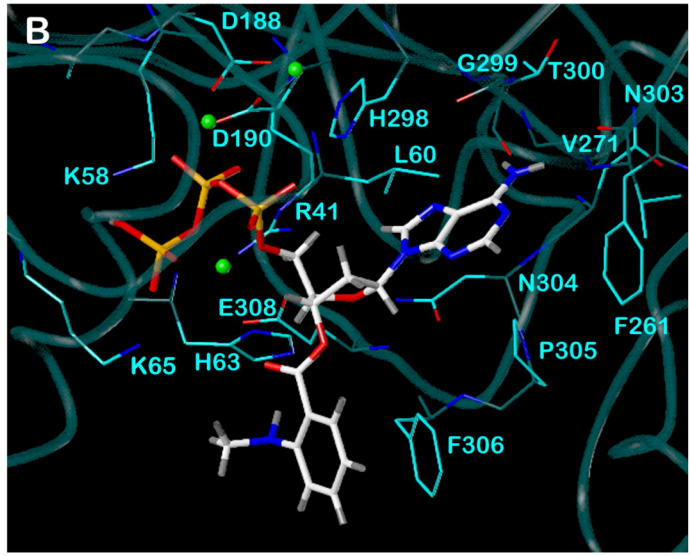
B
D188
G299
T300
N303
H298
D190
V271
L60
K58
R41
N304
E308
F261
P305
K65
H63
F306

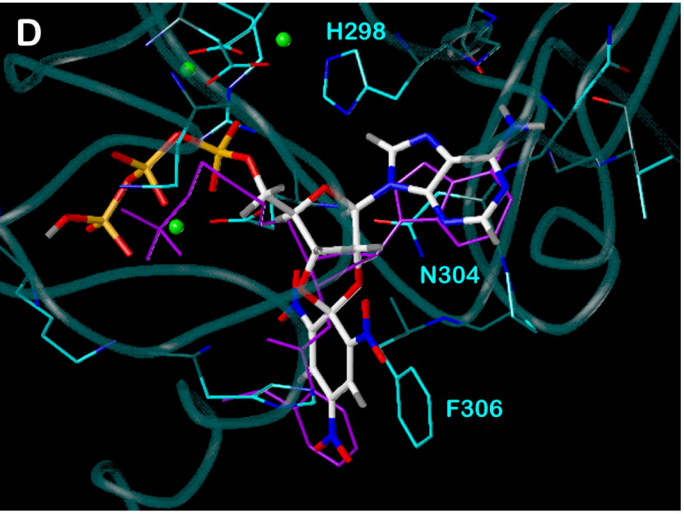
D
H298
N304
F306

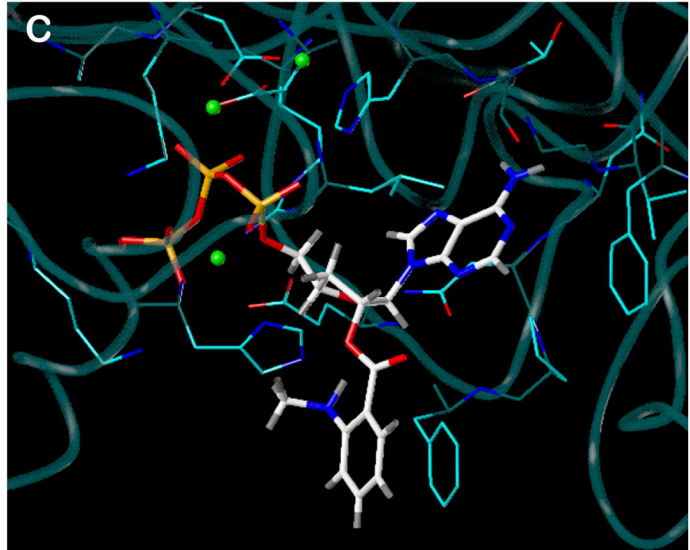
C